

## Impacts of X-ray irradiation on *Saccharomyces cerevisiae* cells growth and physiological-biochemical characteristic\*

CAO Guo-Zhen (曹国珍),<sup>1,2,3</sup> ZHANG Miao-Miao (张苗苗),<sup>1,3</sup> LI Wen-Jian (李文建),<sup>1,2,3</sup>  
MIAO Jian-Shun (缪建顺),<sup>1,3</sup> LU Dong (陆栋),<sup>1,2,3,†</sup> and ZHANG Wen-De (张文德)<sup>4</sup>

<sup>1</sup>*Institute of Modern Physics, Chinese Academy of Sciences, Lanzhou 730000, China*

<sup>2</sup>*School of Pharmacy, Lanzhou University, Lanzhou 730000, China*

<sup>3</sup>*Key Laboratory of Microbial Resources Exploitation and Application, Lanzhou 730000, China*

<sup>4</sup>*Gansu Ronghua Industry Group Co. Ltd, Wuwei 733000, China*

(Received November 4, 2014; accepted in revised form December 22, 2014; published online December 20, 2015)

In this paper, the growth curves of yeast cells exposed to X-rays were detected, and then fitted by Gompertz equation. The yeast cells treated with 50–125 Gy showed an increased exponential growth rate, and lower total biomass at plateau. At doses  $\geq 150$  Gy, cells showed a decreased exponential growth rate and higher total biomass at plateau. DNA lesions were detected by comet assay. Meanwhile, intracellular accumulation of reactive oxygen species (ROS), reduction of mitochondrial membrane potential ( $\Delta\Psi_m$ ) and cell membrane integrity were evaluated. We conclude that X-ray irradiation results in DNA lesions, ROS accumulation and  $\Delta\Psi_m$  decline in a dose-dependent manner, and that these changes may be one of causes of X-rays-induced apoptosis in yeast. Furthermore, yeast cell membrane integrity appeared compromised following irradiation, suggesting that membrane damage may also have a role in the biological effects of radiation.

Keywords: X-rays, *Saccharomyces cerevisiae*, Growth curve, Physiological-biochemical characteristic

DOI: [10.13538/j.1001-8042/nst.26.060302](https://doi.org/10.13538/j.1001-8042/nst.26.060302)

### I. INTRODUCTION

*Saccharomyces cerevisiae*, a kind of industrial microorganism, has been widely applied in fermented industries of wine, beer, and baked foods. As a eukaryotic model organism, the complete genomic sequence of *S. cerevisiae* has been determined. *S. cerevisiae* can be used for studying the relative biological effectiveness (RBE) of ionizing radiations (IR) in higher dose level. Extensive researches [1–4] addressing the adverse effects of IR exposure, using yeast as a model system, have largely been directed toward mutation induction, DNA double-strand break (DSB) repair, and cell cycle effects.

IR absorption by living cells can directly disrupt atomic structures, producing chemical and biological changes. It can also act indirectly through radiolysis of water, thereby generating reactive oxygen species (ROS) that may damage nucleic acids, proteins and cell membrane. An important feature of IR is the spatial distribution of DNA lesions induced as a consequence of energy being deposited unevenly along its track. An X-ray photon deposits most of its energy in a single ionization event, but about 30% of the ionization events are formed closely together leading to the production of clustered damage [5]. IRs also affect the function and structure of cell membranes [6]. This may cause X-ray-induced apoptosis in yeast. Remarkably, the processes occur not only in irradiated cells but also in their progeny [7, 8]. Furthermore, radiation-induced oxidative stress may spread from targeted cells to non-targeted bystander cells through intercellular communication mechanisms [9]. Progeny of the bystander cells also

experience perturbations in oxidative metabolism and exhibit a wide range of oxidative damage [10]. Therefore, the exposure to sublethal doses of IR may affect the process of microorganism growth. Together, the direct and indirect effects of radiation trigger a series of biochemical and molecular signaling events that may repair the damage or culminate in permanent physiological changes or impact to the survival of the progeny or cell death [11].

IR is classified as either electromagnetic or particulate, whereas X-rays belong to electromagnetic radiation, which has been frequently utilized as models of low-linear energy transfer (low-LET) radiation to explore the biological effects of various radiations. Up to now, much work has been reported about yeast destruction induced by X-ray irradiation of certain doses. However, little information is comprehensive and systematic to investigate the effects of growth and physiological-biochemical characteristic. The objective of the current study is to evaluate the impacts of X-ray treatment on yeast growth by measuring and fitting the growth curves according to Gompertz equation and to monitor DNA damage by comet assay. ROS accumulation, mitochondrial membrane potential ( $\Delta\Psi_m$ ) (early signal of apoptosis), and cell membrane integrity were analyzed using flow cytometry with staining 2',7'-dichlorofluorescein diacetate (DCFH-DA), rhodamine123 (Rh123) and propidium iodide (PI), respectively.

### II. MATERIALS AND METHODS

#### A. Strain, medium and growth condition

The *S. cerevisiae* strain used throughout the work is CIC-C 1308 (MATa, budding, haploid) (obtained from the Center of Industrial Culture Collection of China). Yeast cells were

\* Supported by the project of western talent training program of Chinese Academy of Sciences (No. Y306010XB0)

† Corresponding author, [LD@impcas.ac.cn](mailto:LD@impcas.ac.cn)

inoculated in 20 mL yeast peptone dextrose (YPD) medium (1% yeast extract, 2% peptone and 2% glucose), and grown with mechanical oscillation (200 rpm) at 30 °C. In order to optimize the growth, cells were continuously cultured three times. Then, yeast cells were cultured until reaching log phase (about 9 h) to be treated by X-ray irradiation.

### B. X-ray irradiation

The aforementioned yeast cells were divided into eight groups at random. Each group was put into an individual sterilized dish of  $\phi 35$  mm. The samples of the same cell density were irradiated in an ice bath to doses of 0, 25, 50, 75, 100, 125, 150 and 175 Gy with X-rays from an RX-650 X-ray biological irradiator (FAXITRON, USA) operated at 100 kV. The dose rate was 1.5 Gy/min. All samples were treated under the same conditions, except irradiation doses. At the dose rate, the 175 Gy irradiation took 117 min. To exclude the differences in irradiation time, all samples (0–175 Gy) were kept on ice for 117 min. A sham-irradiated control was used as reference.

### C. Determination of yeast cells growth curve

After irradiation, the yeast cells were inoculated into 50 mL YPD medium (inoculum concentration = 1%) to prepare yeast suspension for growth curve determination. The growth curve of yeast was measured by a turbidimetric method. The absorbance values (*OD*) were measured at 600 nm every 3 h to determine the biomass of yeast as described [12]. All the experiments were made in triplicate. The sham-irradiated culture served as control. Afterwards, the data points were fitted by Gompertz equation that can be used to describe the growth characteristics of yeast [13, 14]. The equation is as follows,

$$N = N_0 + be^{-c \cdot \exp(-dt)}, \quad (1)$$

where  $N$  is the total increment in biomass at time  $t$ ;  $N_0$  is the initial cell concentration;  $b$  is the equivalent yeast counts;  $c$  is the early adaptability to growth; and  $d$  is the growth rate constant.

### D. Detection of DNA damage by comet assay

Cell culture of 1 mL was harvested by centrifugation at 5000 rpm, 4 °C for 5 min and washed twice with the same volume of S buffer (1 M sorbitol, 25 mM  $\text{KH}_2\text{PO}_4$ , pH 6.5). The cells were resuspended in 500  $\mu\text{L}$  S buffer, adding 1  $\mu\text{L}$   $\beta$ -mercaptoethanol and 500  $\mu\text{L}$  lyticase (0.5 U/ $\mu\text{L}$ ) at 37 °C, 1 h to obtain spheroplasts. Spheroplasts were collected by centrifugation at 5000 rpm, 4 °C for 5 min, and washed with the same volume of ice-cold S buffer. The comet assay was performed according to the protocol adopted for yeast cells [15, 16]. The pellets were resuspended carefully in the 500  $\mu\text{L}$  1.5% low-melting agarose (w/v in S buffer) at 35 °C.

Then 40  $\mu\text{L}$  of this mixture were spread over a slide coated with a water solution of 0.5% normal-melting agarose, covered with a cover slip, and placed on ice to solidify. After cover slips were removed, the slides were incubated in lysis buffer (30 mM NaOH, 1 M NaCl, 0.05% laurylsarcosine, 50 mM EDTA, 10 mM Tris-HCl, pH 10) for 20 min at 4 °C. Subsequently, the slides were submerged in electrophoresis buffer (30 mM NaOH, 10 mM EDTA, and 10 mM Tris-HCl, pH 10) for 20 min at 4 °C. The samples were then submitted to electrophoresis in the same buffer for 8 min at 0.5 V/cm. After electrophoresis, the slides were incubated in a neutralization buffer (10 mM Tris-HCl, pH 7.4) for 10 min, followed by consecutive incubations in 76% and 96% ethanol and both for 5 min at room temperature. The slides were then air-dried and stained with 20  $\mu\text{L}$  ethidium bromide (EB) (2 mg/mL), covered with a cover slips and analyzed comets by fluorescence microscopy (Olympus BX61, Japan) at  $\times 400$  magnifications, which 50 representative comets of per slide and 6 slides per sample were acquired. The extent of DNA damage was quantified with the help of freeware Cometscore<sup>TM</sup> using index of Olive Tail moment (OTM).

### E. Detection of ROS

Analysis of intracellular ROS was performed with DCFH-DA (Sigma-Aldrich) as described previously [17]. Briefly, DCFH-DA at a final concentration of 10  $\mu\text{M}$  was added to 0.5 mL of cell suspension ( $1 \times 10^7$  cells/mL), followed by incubation at 37 °C for 20 min and then the cells were washed three times with PBS to remove the DCFH-DA, which had not entered the cells. Afterwards, the cells were entered FACSAria II flow cytometer (BD, USA) to measure with an excitation of 488 nm and an emission of  $(530 \pm 15)$  nm (FL1 channel).

### F. Detection of $\Delta\Psi_m$

The assessment of  $\Delta\Psi_m$  was performed utilizing the fluorescent probe Rh123 (Sigma-Aldrich) staining and the procedure as described elsewhere [18]. After X-rays treatment, yeast cells were harvested and washed three times with PBS and incubated with Rh123 at 10  $\mu\text{M}$  for 30 min in the dark. The cells were then recovered, resuspended in 400 mL distilled water and analyzed on the FACSAria II flow cytometer (BD, USA) by the FL1 channel ( $(530 \pm 15)$  nm). The green fluorescence was gated in a scattergram of SSC (side scatter) FSC (forward scatter) in order to include the subpopulation with the highest frequency and homogeneity in the fluorescence measurement.

### G. Detection of cell membrane integrity

Cell membrane permeability was monitored with the PI (Sigma-Aldrich). 0.5 mL of cell suspension

( $1 \times 10^7$  cells/mL) in PBS buffer (pH 7.2), was incubated with PI (in a final concentration of  $10 \mu\text{M}$ ), for 30 min  $30^\circ\text{C}$  in the dark. Subsequently, cells were washed three times with PBS. Analysis was also performed on FACSaria II flow cytometer (BD, USA) and PI was collected in the FL2 channel ( $(620 \pm 15) \text{ nm}$ ).

### H. Reproducibility of the results

All experiments were replicated, independently, at least three times for each radiation doses. Regarding to flow cytometry, the rate was adjusted to keep acquisition at 200 cells per second and a total of 10 000 events were registered per sample. Although, in fluorescence measurements, absolute data were not comparable in the experiments performed on different days, the observed trends were fully consistent among the independent experiments and a typical example is shown. The software FlowJo7.6 was used to analyze flow cytometric data. The data reported for growth curve were the mean  $\pm$ SD of three independent experiments.

## III. RESULTS AND DISCUSSION

### A. Growth curve of yeast

Various kinds of external stresses could significantly impact the yeast growth and the dose effect itself. Low dose microwave favors yeast growth accompanying a repairable increase in cell membrane permeability. The reasons are low-level energy produces molecular transformations and alterations, but the energy is too weak to break down the chemical bonds or primary structure [13, 14, 19]. On the contrary, high dose microwave reduces the yeast growth or directly lead to cell death.

To examine the X-ray effects on yeast growth, yeast cells in the mid-exponential phase were irradiated by X-rays and then inoculated to 50 mL fresh YPD medium to analyze the growth curve using  $OD_{600}$  which represents the yeast biomass [12]. As shown in Fig. 1, the yeast biomass increased gradually with the time of culturing. The cells entered the logarithmic phase after about 3 h and reached the post-diauxic phase at around 18 h. Then they finally passed into the stationary phase when the biomass decreased slightly. At 25 Gy dose, the process of yeast growth is almost similar to the sham-irradiated control, as 25 Gy is too low to produce a significant impact on yeast cells. However, the 50–125 Gy treatments resulted in a longer pre-exponential lag and rapid exponential growth rate than sham-irradiated control. Moreover, the 50–125 Gy irradiated cells showed a much earlier diauxic shift (DS) and a consequent reduction of their total biomass at plateau. At 150 and 175 Gy, we observed a significantly reduced exponential growth rate, a delayed DS and an increase of the total biomass at plateau. The time of half log phase and plateau phase were investigated and presented in Table 1.

Gompertz equation was used to fit the growth curve, with a good fitting coefficient (data not shown). This indicates

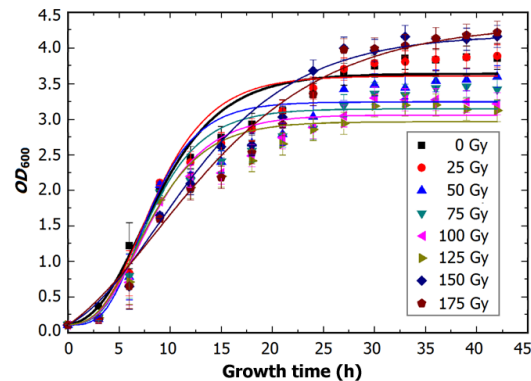


Fig. 1. (Color online) Growth curves of yeast cells after X-rays treatment of various doses.  $OD$  were determined at 600 nm every 3 h to measure the concentration of yeast cells, and was fitted by Gompertz function. Each point represents the mean of results of three independent experiments; standard deviations are presented.

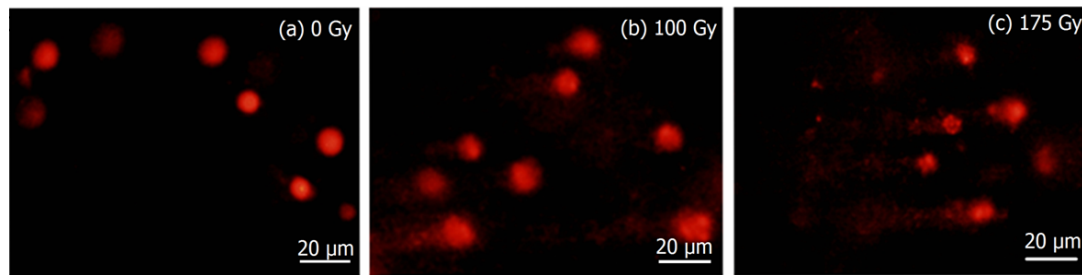
TABLE 1. The time of half log and plateau phases of yeast cell growth

Dose (Gy)	Time (h)	
	Half log phase	Plateau phase
0	$8.91 \pm 0.61$	$17.81 \pm 1.17$
25	$8.69 \pm 0.54$	$17.39 \pm 1.01$
50	$8.27 \pm 1.11$	$16.54 \pm 2.16$
75	$7.85 \pm 0.77$	$15.69 \pm 1.54$
100	$8.06 \pm 0.64$	$16.12 \pm 1.29$
125	$7.64 \pm 1.04$	$15.27 \pm 2.08$
150	$14.21 \pm 1.45$	$28.42 \pm 2.89$
175	$14.42 \pm 1.61$	$28.84 \pm 3.18$

that the growth characteristics of yeast can be well described by the Gompertz equation. According to the equation, the coefficients of  $N_0$ ,  $b$ ,  $c$  and  $d$  at different doses were obtained (Table 2). The growth rate constant,  $d$ , increased with the dose from 50–125 Gy, as compared with the sham-irradiated control. The total biomass of yeast,  $b$ , decreased with increasing the dose from 125 Gy, but it increased with the dose from 150–175 Gy. These indicate that X-ray irradiation make the growth rate of yeast cells increase in dose range of 50–125 Gy, but biomass at plateau appears reduced. At 150 Gy and 175 Gy, the growth rate reduced, the DS delayed and the total mass at plateau increased consequently. These phenomena can be rationalized by previous transcriptomic studies. At lower doses of X-ray irradiation, yeast cells are perfectly viable and proliferating, inducing a set of genes involved in response to oxidation, glucose metabolism, DNA repair and protein synthesis [20]. At 170 Gy, however, in spite of an induced 45% mortality and an efficient cell cycle arrest in G2, the irradiation is less effective in inducing anti-oxidative genes, histone and protein synthesis genes [21]. It is therefore likely that yeast cells irradiated to lower doses in the expanded lag can accumulate proteins, which are required for a more efficient growth in oxidative conditions. They have a more efficient glucose consumption and therefore reach the DS earlier, typically with lower total biomass; while at high-

TABLE 2. Values of  $N_0$ ,  $b$ ,  $c$  and  $d$  in yeast cell growth, derived from Gompertz equation

Dose(Gy)	Parameters of Gompertz equation			
	$N_0$	$b$	$c$	$D$
0	$0.081 \pm 0.010$	$3.560 \pm 0.102$	$5.001 \pm 0.206$	$0.229 \pm 0.012$
25	$0.098 \pm 0.015$	$3.512 \pm 0.128$	$6.202 \pm 1.702$	$0.260 \pm 0.034$
50	$0.102 \pm 0.004$	$3.142 \pm 0.128$	$8.465 \pm 2.402$	$0.316 \pm 0.038$
75	$0.105 \pm 0.011$	$3.042 \pm 0.116$	$6.978 \pm 0.140$	$0.288 \pm 0.039$
100	$0.097 \pm 0.013$	$2.963 \pm 0.103$	$6.134 \pm 1.975$	$0.266 \pm 0.039$
125	$0.098 \pm 0.017$	$2.867 \pm 0.107$	$5.990 \pm 2.126$	$0.262 \pm 0.043$
150	$-0.080 \pm 0.158$	$4.275 \pm 0.306$	$3.146 \pm 0.800$	$0.132 \pm 0.024$
175	$-0.272 \pm 0.338$	$4.620 \pm 0.578$	$2.508 \pm 0.784$	$0.106 \pm 0.025$

Fig. 2. (Color online) Fluorescence images (at  $\times 400$  magnification) from yeast comet assays in the cells irradiated to 0, 100 and 175 Gy.

er doses, proliferation is impaired and  $DS$  is delayed with a higher total mass at plateau.

### B. DNA damage induced by X-rays

It is well known that IR can result in DNA damage by directly physical effect and indirectly  $ROS$ , which are generated at localized regions in the nucleus. IR possess extensive broadness and manners of different DNA lesions that can cause structural damage to the DNA molecule and can alter or eliminate the cell's ability of gene transcription [22]. Of the total DNA lesions induced by IR, 80% are base modifications and 20% are sugar phosphate backbone damage [23]. Forms of DNA damage include double-strand or single-strand breaks (DSBs or SSBs), cross-links, oxidative base modification and clustered base damage. Regarding to the numbers of DNA lesions, one Gy IR have been estimated to be approximately 1000 base modifications, 1000 SSBs, 40 DSBs, 20 DNA-DNA cross-links, 150 DNA-protein cross-links and 160-320 non-DSB clustered DNA damage per cell [24–26]. SSBs have lower biological impact since they are readily repaired using the opposite strand as a template, whereas DSBs are thought to be much more deleterious and occur when the two strands simultaneously break in close positions.

In order to quantify DNA damage of yeast cells exposed to X-rays, comet assay was applied in experimental conditions optimized for making detection of DNA damage more sensitive. For the quantitative index, we used  $OTM$  as a sensitive parameter for comet assay using a single cell species with a uniform DNA pattern and could evaluate a wide extent of DNA damage. Quantification of DNA damage ( $OTM$ ) in yeast cells irradiated to 0, 25, 50, 75, 100, 125, 150 and 175 Gy, are

$0.74 \pm 1.2^*$ ,  $1.5 \pm 1.3^{*\#}$ ,  $2.4 \pm 1.0^{*\#}$ ,  $4.2 \pm 2.2^{*\#}$ ,  $6.5 \pm 1.8^{*\#}$ ,  $6.9 \pm 2.1^{*\$}$ ,  $8.5 \pm 3.1^{*\#}$  and  $13.7 \pm 2.9^{*\#}$  (At least 300 comets per experiment. \*:  $p < 0.01$  vs. control; \$, #:  $p < 0.05$  and  $p < 0.01$  vs. prior group.). The results show that the DNA damage induced in yeast cells exposed to different doses of X-rays clearly increased with dose ( $p < 0.05$  or  $p < 0.01$ ). However, the increase of X-ray irradiation-induced DSBs follow a linear relationship in yeast cells [4], suggesting that the generation of DSBs may be more regular than total DNA damage in X-ray irradiated yeast cells. Similar results were observed by visual inspection of cell comet images at 100 and 175 Gy (Fig. 2), and the extent of damage also appears aggravated with the increase of X-ray irradiation doses.

### C. ROS production induced by X-rays

In cells irradiated by X-rays, energy deposition causes endogenous bursts of  $ROS$  along the radiation track and in the intercellular matrix due to the effects of water radiolysis, and the track structure determines the relative potency of biological effects of different radiations [27, 28]. It is well documented that the intracellular production of  $ROS$  causes cell damage. As a result, different signaling cascades responding to the stress conditions are triggered [29]. Also,  $ROS$ , as cell death regulators, has been linked with the phenomenon of apoptosis in yeast cells [30, 31].

To investigate the  $ROS$  accumulation in X-ray-induced yeast cells, we determined  $ROS$  with DCFH-DA, which enters the live cell and emits green fluorescence as is oxidized by  $ROS$  [32]. In quantification  $ROS$  production, flow cytometric analysis (Fig. 3, histograms) showed that the subpopulation of positive cells with signal intensity over a threshold



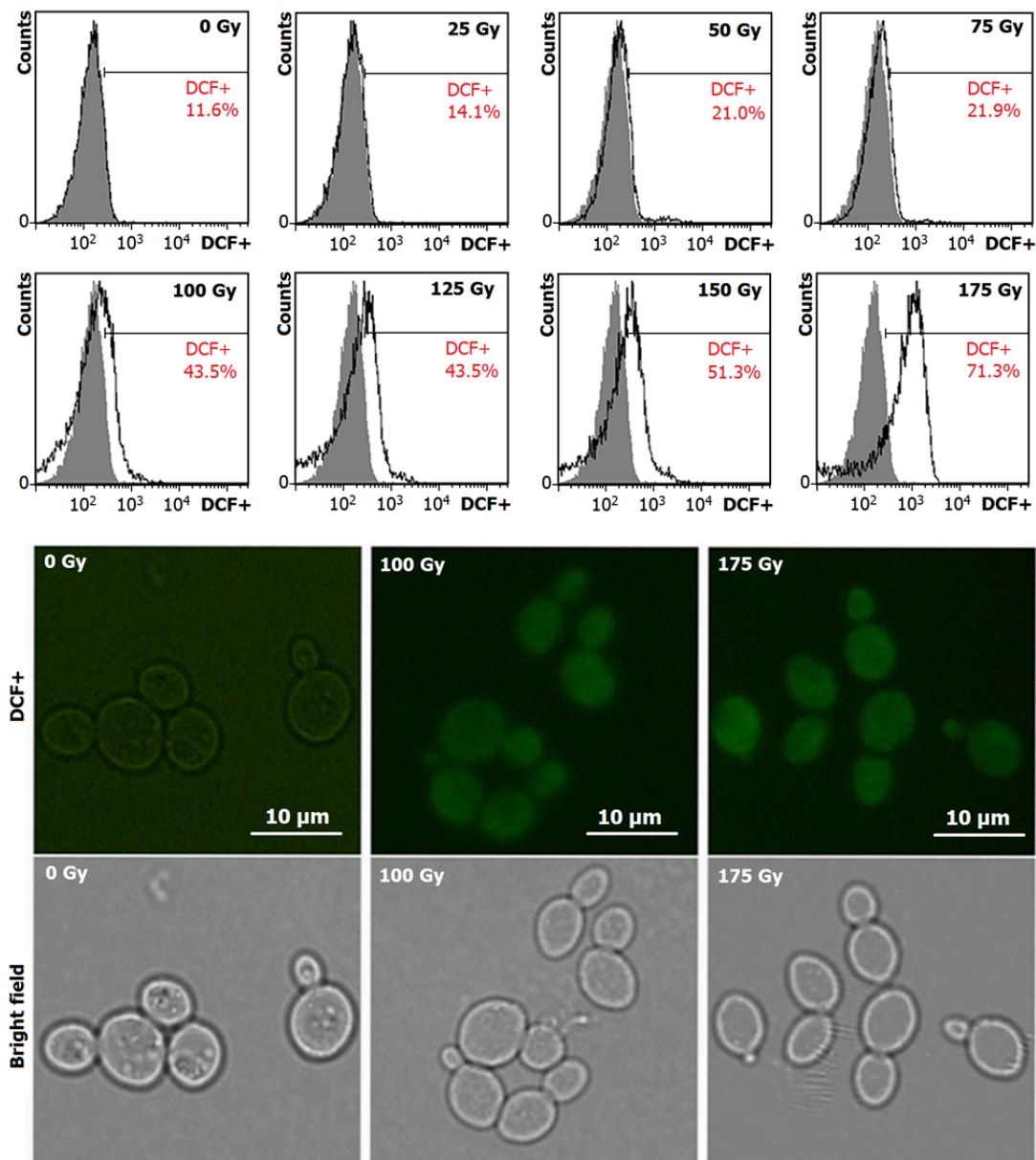


Fig. 3. (Color online) *ROS* accumulation in yeast cells irradiated to different doses by X-rays. The histograms are flow cytometry analyses of production of *ROS* determined by DCFH-DA labeling, with the grey histograms being the control. The images are visualization of *ROS* production in yeast cells irradiated to 0 Gy (control), 100 Gy and 175 Gy by X-rays, and stained with DCFH-DA, with the upper panel being fluorescence micrographs of incorporated Rh123, and the lower panel being phase contrast micrographs of the same cells.

value increased from  $\sim 11.6\%$  at 0 Gy to  $\sim 71.3\%$  at 175 Gy, in a well dose-dependent manner, i.e. the burst of *ROS* is proportional to the radiation dose. The microscopy observations of cells of 100 or 175 Gy showed a strong green fluorescence (Fig. 3, the upper images), indicating considerable amounts of *ROS* in the cells; while the control cells showed no fluorescence. These indicate that X-ray irradiation cause intracellular accumulation of *ROS*, causing induced damages in the yeast cells. The results are corresponding to the changes of anti-oxidative genes transcriptional described Ref. [20]. *ROS* levels show similar dose effect of DNA dam-

age (Fig. 2). Thus, it can be argued that the increased *ROS* level is responsible for the loss of activity and production of DNA lesions in yeast cells exposed to X-rays.

#### D. X-ray irradiation decrease $\Delta\Psi_m$

The mitochondria play an important role in yeast respiratory chain and energy coupling. And it was reported that mitochondrial involved apoptosis in yeast [33]. Mitochondria are well known as the primary coordinators of apoptot-

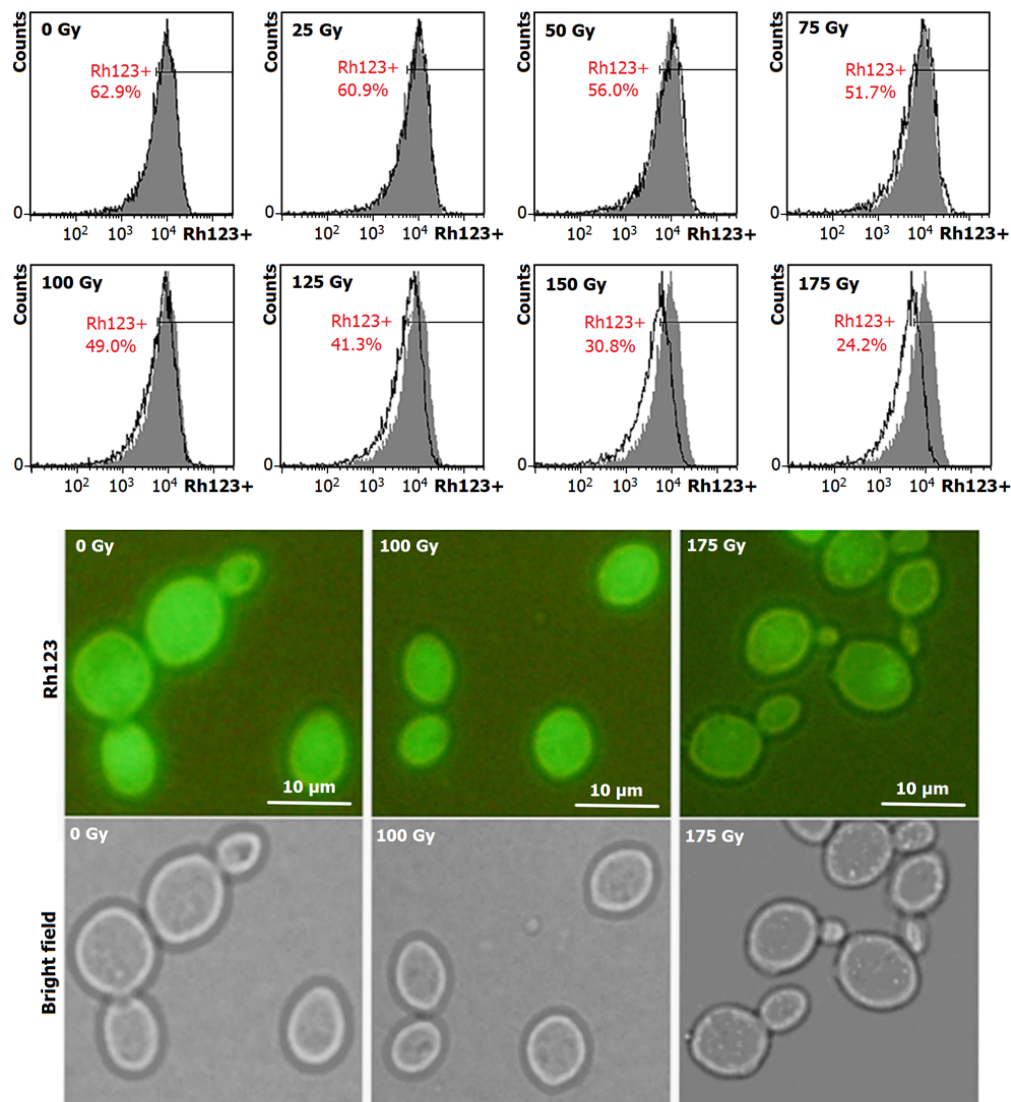


Fig. 4. (Color online) Change of  $\Delta\Psi_m$  in yeast cells irradiated by different doses X-rays. The histograms are from flow cytometry analyses of  $\Delta\Psi_m$  in the yeast cells stained with Rh123, with the grey histograms being the control. The fluorescence images are taken from yeast cells stained with Rh123 after treatment of 0, 100 and 175 Gy, with the upper panel being fluorescence micrographs of incorporated Rh123, and the lower panel being phase contrast micrographs of the same cells.

ic processes to control the intrinsic apoptotic pathway [34], and the dissipation of  $\Delta\Psi_m$  is an early event in the apoptosis [35, 36]. Moreover,  $\Delta\Psi_m$  is also an indicator of the mitochondrial membrane integrity, which would depolarize when the membrane is perturbed, combining with less fluorescence probe [37].

The generation of *ROS* is an upstream event of  $\Delta\Psi_m$  decreasing. Therefore, we detected  $\Delta\Psi_m$  in yeast cells treated by X-rays. The yeast cells were incubated with Rh123, a fluorescent dye that specifically stains active mitochondria in living cells. The changes of Rh123 distribution in cells indicate variations in the  $\Delta\Psi_m$  [38]. As shown in Fig. 4, compared with the 0 Gy cells,  $\Delta\Psi_m$  of the irradiated yeast cells decreased with increasing doses of 25–175 Gy, with the percentage of the positive rate of Rh123 being 60.9% at 0 Gy

and 24.2% at 175 Gy. Similarly, the fluorescence intensity of green fluorescence in the 100 and 175 Gy-treated cells decreased with increasing doses, and 175 Gy-treated cells was weaker than the 100 Gy-treated cells, confirming the  $\Delta\Psi_m$  disruption in X-rays-treated cells. Our results show that the production of *ROS* is accompanied by a reduction of  $\Delta\Psi_m$  in yeast cells treated with X-rays. The observations demonstrate that X-ray irradiation can result in depolarization of  $\Delta\Psi_m$  because of the intracellular accumulation of *ROS* and cause the opening of the mitochondrial permeability transition pore and mitochondrial swelling which eventually leads to the dysfunction of mitochondria.

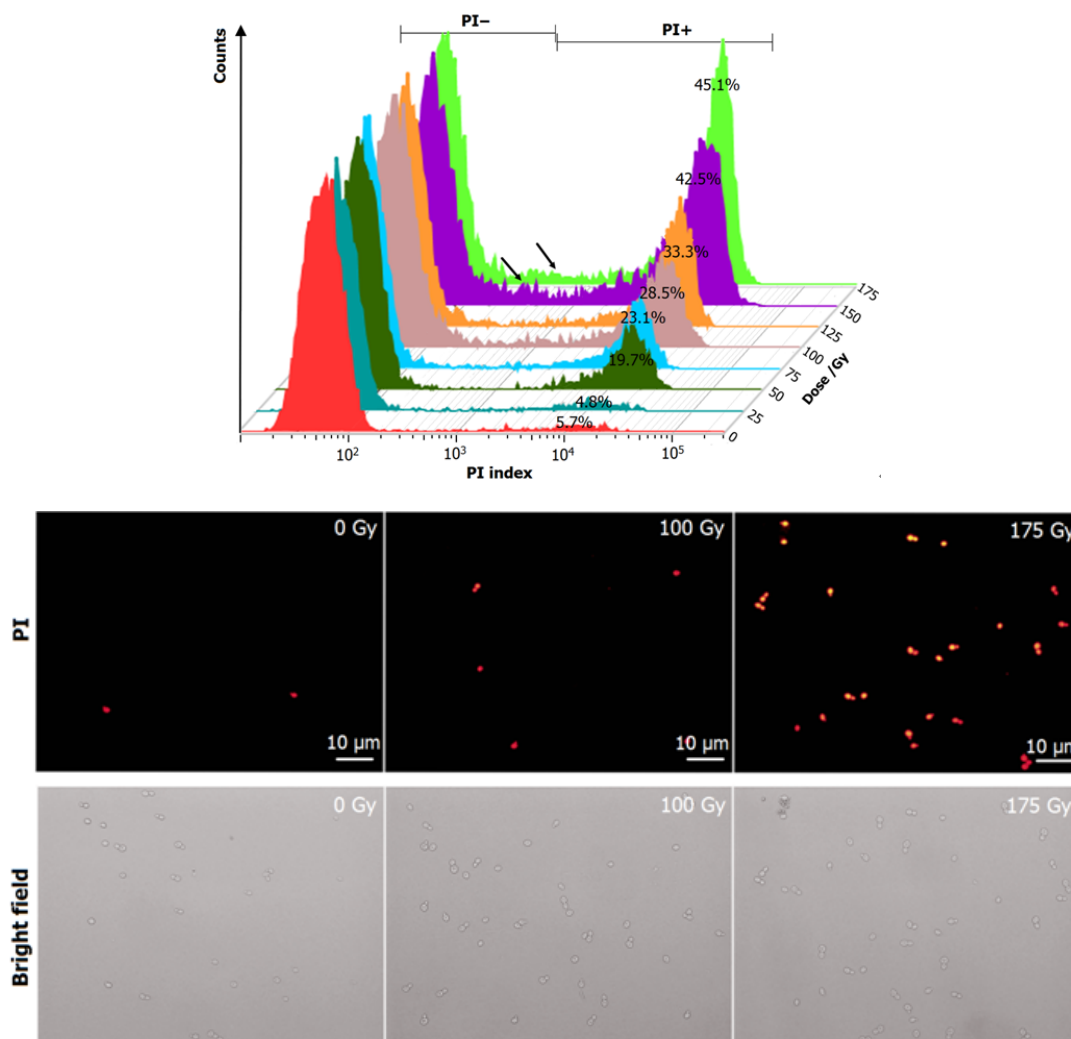


Fig. 5. (Color online) Changes in cell membrane permeability in yeast cells irradiated to different doses by X-rays. The histograms are from flow cytometry analyses of cell membrane permeability evaluated by PI marking, with the rate of PI+ representing changes in permeability. The images are visualization of cell membrane permeability in PI-stained yeast cells treated at 0, 100 and 175 Gy, with the upper panel being fluorescence micrographs of incorporated PI, and the lower panel being phase contrast micrographs of the same cells.

#### E. Change of cell membrane integrity induced by X-rays

Research into the molecular mechanisms of the lesions of IR on organisms has been focused on complex, irreparable clustered DNA damage and deletion or insertion of single or multiple DNA bases [39]. Comparatively, the IR effects on yeast cell membranes have not been considered with enough attention, despite the fact that, as a physiological barrier, the cell membrane may be damaged due to the interaction between X-ray photons and biological macromolecules of the membrane. The effects on cell membranes may be a reason for X-ray irradiation caused yeast apoptosis or cell death. The damage of cell membranes leads to changes of permeability or integrity, which can be measured by the uptake rate of PI (Fig. 5). PI is a nucleotide-binding probe used extensively to assess the membrane integrity. PI can freely penetrate to the cell interior and combine with DNA [40, 41]. As shown in Fig. 5, the numbers of the uptake PI cells (permeabilized

cells) increased after X-rays irradiation, which indicated that other targets could also be more vital to X-rays irradiation inactivation than DNA.

#### IV. CONCLUSION

The effects of X-rays exposure on *S. cerevisiae* cells growth and physiological-biochemical characteristic were investigated, including DNA damage, ROS accumulation and the changes of  $\Delta\Psi_m$  and cell membrane integrity. Relatively low doses of X rays irradiation (25–125 Gy) resulted in an increase of pre-exponential phase lag and of exponential growth rate. In the same range of doses we observed an earlier *DS* and a decrease of the total biomass at plateau. On the other end at higher doses (150 and 175 Gy), growth rate is decreased and *DS* is delayed with increased total biomass

at plateau. At the same time, X-ray irradiation led to the DNA lesions, intracellular *ROS* accumulation and  $\Delta\Psi_m$  decrease in a dose-dependent manner. These damage or impacts are also mainly cause X-rays induce yeast apoptosis or cell death. Moreover, our present study demonstrated that X-ray irradiation could destroy cell membrane integrity to a great extent. These results, which are in agreement with the observed increase of ergosterol biosynthesis genes upon X-rays irradiation [20], suggest that other targets besides DNA are damaged by radiation and may have a deep impact on the cell physiology.

In conclusion, the results of the present study strongly suggest that X-ray irradiation could cause multiple effects on yeast cell and that the extent of the effects depend on dose level. These insights may provide fundamental data and useful information for the irradiation investigation of microorganisms. However, the relative mechanisms, for instance those responsible for the changes in growth rate and the role of the cell membrane integrity impacted by X-ray irradiation, remain to be elucidated at the molecular level and further studies will be needed.

- [1] Bennett C B, Lewis L K, Karthikeyan G, *et al.* Genes required for ionizing radiation resistance in yeast. *Nat Genet*, 2001, **29**: 426–434. DOI: [10.1038/ng778](https://doi.org/10.1038/ng778)
- [2] Clerici M, Mantiero D, Lucchini G, *et al.* The *Saccharomyces cerevisiae* Sae2 protein promotes resection and bridging of double strand break ends. *J Biol Chem*, 2005, **280**: 38631–38638. DOI: [10.1074/jbc.M508339200](https://doi.org/10.1074/jbc.M508339200)
- [3] Brunborg G, Resnick M A and Williamson D H. Cell-cycle-specific repair of DNA double-strand breaks in *Saccharomyces cerevisiae*. *Radiat Res*, 1980, **82**: 547–558. DOI: [10.2307/3575321](https://doi.org/10.2307/3575321)
- [4] Illner D and Scherthan H. Ionizing irradiation-induced radical stress stalls live meiotic chromosome movements by altering the actin cytoskeleton. *P Natl Acad Sci USA*, 2013, **110**: 16027–16032. DOI: [10.1073/pnas.1306324110](https://doi.org/10.1073/pnas.1306324110)
- [5] Eccles L J, O'Neill P and Lomax M E. Delayed repair of radiation induced clustered DNA damage: Friend or foe? *Mutat Res-Fund Mol M*, 2011, **711**: 134–141. DOI: [10.1016/j.mrfmmm.2010.11.003](https://doi.org/10.1016/j.mrfmmm.2010.11.003)
- [6] Corre I, Niaudet C and Paris F. Plasma membrane signaling induced by ionizing radiation. *Mutat Res-Rev Mutat*, 2010, **704**: 61–67. DOI: [10.1016/j.mrrev.2010.01.014](https://doi.org/10.1016/j.mrrev.2010.01.014)
- [7] Kryston T B, Georgiev A B, Pissis P, *et al.* Role of oxidative stress and DNA damage in human carcinogenesis. *Mutat Res-Fund Mol M*, 2011, **711**: 193–201. DOI: [10.1016/j.mrfmmm.2010.12.016](https://doi.org/10.1016/j.mrfmmm.2010.12.016)
- [8] Tamminga J and Kovalchuk O. Role of DNA damage and epigenetic DNA methylation changes in radiation-induced genomic instability and bystander effects in germline in vivo. *Current Mol Pharmacol*, 2011, **4**: 115–125. DOI: [10.2174/1874467211104020115](https://doi.org/10.2174/1874467211104020115)
- [9] Hei T K, Zhou H, Chai Y, *et al.* Radiation induced non-targeted response: mechanism and potential clinical implications. *Current Mol Pharmacol*, 2011, **4**: 96–105. DOI: [10.2174/1874467211104020096](https://doi.org/10.2174/1874467211104020096)
- [10] Buonanno M, de Toledo S M, Pain D, *et al.* Long-term consequences of radiation-induced bystander effects depend on radiation quality and dose and correlate with oxidative stress. *Radiat Res*, 2011, **175**: 405–415. DOI: [10.1667/RR2461.1](https://doi.org/10.1667/RR2461.1)
- [11] Spitz D R, Azzam E I, Li J J, *et al.* Metabolic oxidation/reduction reactions and cellular responses to ionizing radiation: a unifying concept in stress response biology. *Cancer Metastasis Rev*, 2004, **23**: 311–322. DOI: [10.1023/B:CANC.0000031769.14728.bc](https://doi.org/10.1023/B:CANC.0000031769.14728.bc)
- [12] Cao G Z, Miao J S, Zhang M M, *et al.* The research of measuring *Saccharomyces cerevisiae* cells concentration by spectrophotometry. *China Brewing*, 2014, **33**: 129–133. (in Chinese) DOI: [10.3969/j.issn.0254-5071.2014.04.031](https://doi.org/10.3969/j.issn.0254-5071.2014.04.031)
- [13] Zeng S W, Huang Q L and Zhao S M. Effects of microwave irradiation dose and time on Yeast ZSM-001 growth and cell membrane permeability. *Food Control*, 2014, **46**: 360–367. DOI: [10.1016/j.foodcont.2014.05.053](https://doi.org/10.1016/j.foodcont.2014.05.053)
- [14] Fang Y P, Hu J, Xiong S B, *et al.* Effect of low-dose microwave radiation on *Aspergillus parasiticus*. *Food Control*, 2011, **22**: 1078–1084. DOI: [10.1016/j.foodcont.2011.01.004](https://doi.org/10.1016/j.foodcont.2011.01.004)
- [15] Azevedo F, Marques F, Fokt H, *et al.* Measuring oxidative DNA damage and DNA repair using the yeast comet assay. *Yeast*, 2011, **28**: 55–61. DOI: [10.1002/yea.1820](https://doi.org/10.1002/yea.1820)
- [16] Litwin I, Bocér T, Dziadkowiec D, *et al.* Oxidative stress and replication-independent DNA breakage induced by arsenic in *Saccharomyces cerevisiae*. *PLoS Genet*, 2013, **9**: 1003640. DOI: [10.1371/journal.pgen.1003640](https://doi.org/10.1371/journal.pgen.1003640)
- [17] Wu J, Min R, Wu M, *et al.* Gefitinib induces mitochondrial-dependent apoptosis in *Saccharomyces cerevisiae*. *Mol Med Rep*, 2011, **4**: 357–362. DOI: [10.3892/mmr.2011.427](https://doi.org/10.3892/mmr.2011.427)
- [18] Sapienza K, Bannister W and Balzan R. Mitochondrial involvement in aspirin-induced apoptosis in yeast. *Microbiology*, 2008, **154**: 2740–2747. DOI: [10.1099/mic.0.2008/017228-0](https://doi.org/10.1099/mic.0.2008/017228-0)
- [19] Xiang B, Sundararajan S, Mis Solval K, *et al.* Effects of pulsed electric fields on physicochemical properties and microbial inactivation of carrot juice. *J Food Process Preserv*, 2014, **38**: 1556–1564. DOI: [10.1111/jfpp.12115](https://doi.org/10.1111/jfpp.12115)
- [20] Sacerdot C, Mercier G, Todeschini A L, *et al.* Impact of ionizing radiation on the life cycle of *Saccharomyces cerevisiae* Ty1 retrotransposon. *Yeast*, 2005, **22**: 441–455. DOI: [10.1002/yea.1222](https://doi.org/10.1002/yea.1222)
- [21] Gasch A P, Huang M, Metzner S, *et al.* Genomic expression responses to DNA-damaging agents and the regulatory role of the yeast ATR homolog Mec1p. *Mol Biol Cell*, 2001, **12**: 2987–3003. DOI: [10.1091/mbc.12.10.2987](https://doi.org/10.1091/mbc.12.10.2987)
- [22] Martin L M, Marples B, Coffey M, *et al.* DNA mismatch repair and the DNA damage response to ionizing radiation: Making sense of apparently conflicting data. *Cancer Treat Rev*, 2010, **36**: 518–527. DOI: [10.1016/j.ctrv.2010.03.008](https://doi.org/10.1016/j.ctrv.2010.03.008)
- [23] Cadet J, Delatour T, Douki T, *et al.* Hydroxyl radicals and DNA base damage. *Mutat Res-Fund Mol M*, 1999, **424**: 9–21. DOI: [10.1016/S0027-5107\(99\)00004-4](https://doi.org/10.1016/S0027-5107(99)00004-4)
- [24] Goodhead D T. Initial events in the cellular effects of ionizing radiations: clustered damage in DNA. *Int J Radiat Biol*, 1994, **65**: 7–17. DOI: [10.1080/09553009414550021](https://doi.org/10.1080/09553009414550021)
- [25] Nikjoo H, Uehara S, Wilson W E, *et al.* Track structure in radiation biology: theory and applications. *Int J Radiat Biol*, 1998, **73**: 355–364. DOI: [10.1080/095530098142176](https://doi.org/10.1080/095530098142176)
- [26] Rothkamm K and Löbrich M. Evidence for a lack of DNA



- double-strand break repair in human cells exposed to very low x-ray doses. *P Natl Acad Sci USA*, 2003, **100**: 5057–5062. DOI: [10.1073/pnas.0830918100](https://doi.org/10.1073/pnas.0830918100)
- [27] Draganić I G. Radiolysis of water: a look at its origin and occurrence in the nature. *Radiat Phys Chem*, 2005, **72**: 181–186. DOI: [10.1016/j.radphyschem.2004.09.012](https://doi.org/10.1016/j.radphyschem.2004.09.012)
- [28] Goodhead D T. Energy deposition stochastics and track structure: what about the target? *Radiat Prot Dosimetry*, 2006, **122**: 3–15. DOI: [10.1093/rpd/ncl498](https://doi.org/10.1093/rpd/ncl498)
- [29] de Toledo S M, Asaad N, Venkatachalam P, *et al.* Adaptive responses to low-dose/low-dose-rate  $\gamma$  rays in normal human fibroblasts: The role of growth architecture and oxidative metabolism. *Radiat Res*, 2006, **166**: 849–857. DOI: [10.1667/RR0640.1](https://doi.org/10.1667/RR0640.1)
- [30] Carmona-Gutierrez D, Eisenberg T, Buttner S, *et al.* Apoptosis in yeast: triggers, pathways, subroutines. *Cell Death Differ*, 2010, **17**: 763–773. DOI: [10.1038/cdd.2009.219](https://doi.org/10.1038/cdd.2009.219)
- [31] Perrone G G, Tan S X and Dawes I W. Reactive oxygen species and yeast apoptosis. *Biochim Biophys Acta*, 2008, **1783**: 1354–1368. DOI: [10.1016/j.bbamcr.2008.01.023](https://doi.org/10.1016/j.bbamcr.2008.01.023)
- [32] Silva R D, Sotoca R, Johansson B, *et al.* Hyperosmotic stress induces metacaspase-and mitochondria-dependent apoptosis in *Saccharomyces cerevisiae*. *Mol Microbiol*, 2005, **58**: 824–834. DOI: [10.1111/j.1365-2958.2005.04868.x](https://doi.org/10.1111/j.1365-2958.2005.04868.x)
- [33] Sapienza K, Bannister W and Balzan R. Mitochondrial involvement in aspirin-induced apoptosis in yeast. *Microbiology*, 2008, **154**: 2740–2747. DOI: [10.1099/mic.0.2008/017228-0](https://doi.org/10.1099/mic.0.2008/017228-0)
- [34] Hengartner M O. The biochemistry of apoptosis. *Nature*, 2000, **407**: 770–776. DOI: [10.1038/35037710](https://doi.org/10.1038/35037710)
- [35] Du L, Yu Y, Chen J, *et al.* Arsenic induces caspase-and mitochondria-mediated apoptosis in *Saccharomyces cerevisiae*. *FEMS Yeast Res*, 2007, **7**: 860–865. DOI: [10.1111/j.1567-1364.2007.00274.x](https://doi.org/10.1111/j.1567-1364.2007.00274.x)
- [36] Pozniakovsky A I, Knorre D A, Markova O V, *et al.* Role of mitochondria in the pheromone-and amiodarone-induced programmed death of yeast. *J Cell Biol*, 2005, **168**: 257–269. DOI: [10.1083/jcb.200408145](https://doi.org/10.1083/jcb.200408145)
- [37] Ma R N, Feng H Q, Liang Y D, *et al.* An atmospheric-pressure cold plasma leads to apoptosis in *Saccharomyces cerevisiae* by accumulating intracellular reactive oxygen species and calcium. *J Phys D Appl Phys*, 2013, **46**: 285401. DOI: [10.1088/0022-3727/46/28/285401](https://doi.org/10.1088/0022-3727/46/28/285401)
- [38] Ludovico P, Sansonetty F and Côte-Rea M. Assessment of mitochondrial membrane potential in yeast cell populations by flow cytometry. *Microbiology*, 2001, **147**: 3335–3343. DOI: [10.1099/00221287-147-12-3335](https://doi.org/10.1099/00221287-147-12-3335)
- [39] Terato H and Ide H. Clustered DNA damage induced by heavy ion particles. *Soc Biol Sci space*, 2004, **18**: 206–215. DOI: [10.2187/bss.18.206](https://doi.org/10.2187/bss.18.206)
- [40] Mannazzu I, Angelozzi D, Belviso S, *et al.* Behaviour of *Saccharomyces cerevisiae* wine strains during adaptation to unfavourable conditions of fermentation on synthetic medium: cell lipid composition, membrane integrity, viability and fermentative activity. *Int J Food Microbiol*, 2008, **121**: 84–91. DOI: [10.1016/j.ijfoodmicro.2007.11.003](https://doi.org/10.1016/j.ijfoodmicro.2007.11.003)
- [41] Marza E, Camougrand N and Manon S. Bax expression protects yeast plasma membrane against ethanol-induced permeabilization. *FEBS Lett*, 2002, **521**: 47–52. DOI: [10.1016/S0014-5793\(02\)02819-3](https://doi.org/10.1016/S0014-5793(02)02819-3)